Conference paper

Alena Michalcová*, Ivo Marek, Adél Len, Oleg Heczko, Jan Drahokoupil, Dalibor Vojtěch, Štěpán Huber and Radka Nováková

Structure and properties of nanocrystalline nickel prepared by selective leaching at different temperatures

DOI 10.1515/pac-2016-1028

Abstract: Nanocrystalline nickel is an interesting material for catalysis, and also, like all nanocrystalline metals, it has potential for structural application. Our aim was to develop a method for preparation of precursor materials for powder metallurgy. Because of this, selective leaching of binary alloy was chosen as it leads to production of nanocrystalline clustered (sub)micro particles. In this work, the preparation of Ni particles by selective leaching of Al matrix from Al-50 wt.% Ni in NaOH water solution is described. It was found that structure and magnetic properties were strongly dependent on leaching temperature, which was proven by characterization of Ni particles leached at – 20, 0, 20, 40, 60 and 80 °C. The microstructure of as-prepared particles was observed by HRTEM and also by small angle neutron scattering. Magnetic properties were characterized by measuring of saturation magnetization. It was proven that with increased leaching temperature the grain size of prepared nanocrystalline particles increased. Also the value of saturated magnetization follows the same trend. The amount of hydrogen stored in nickel particles is independent on leaching temperature.

Keywords: magnetic properties; magnetization; nanocrystals; neutron scattering; nickel; SANS; SSC-2016; X-ray diffraction.

Introduction

Metallic nanoparticles [1] and especially nickel nanoparticles have [2, 3] wide application potential in chemical catalysis. On the top, they can be used as powder precursors for powder metallurgical preparation of bulk materials with ultra-fine structure [3]. Nickel nanoparticles can be prepared from solution of nickel salt by chemical reduction [4–10] or reduction by gamma irradiation [11]. Nickel chemical reduction e.g. by hydrazine is performed in ethylene glycol environment [12], which brings the need of cleaning the nickel nanoparticles before utilization. Because of this reason, obtaining of Ni particles by selective leaching of

Article note: A collection of invited papers based on presentations at the 12th Conference on Solid State Chemistry (SSC-2016), Prague, Czech Republic, 18–23 September 2016.

***Corresponding author: Alena Michalcová**, University of Chemistry and Technology, Prague, Department of Metals and Corrosion Engineering, Technická 5, 166 28 Prague 6, Czech Republic, e-mail: michalca@vscht.cz
Ivo Marek, Dalibor Vojtěch and Radka Nováková: University of Chemistry and Technology, Prague, Department of Metals and Corrosion Engineering, Technická 5, 166 28 Prague 6, Czech Republic
Adél Len: Budapest Nuclear Centre, Hungarian Academy of Sciences, Association of the KFKI Research Institutes Centre for Energy Research – Wigner Research Centre for Physics, H-1525 Budapest 114, P.O.B. 49, Hungary
Oleg Heczko and Jan Drahokoupil: Institute of Physics of the ASCR, v. v. i., Na Slovance 2, 182 21 Praha, Czech Republic
Štěpán Huber: University of Chemistry and Technology, Prague, Department of Inorganic Chemistry, Technická 5, 166 28 Prague 6, Czech Republic

Al–Ni alloys in NaOH water solution is very promising. Selective leaching method is a process consisting of preparation of binary alloy in form of supersaturated solid solution and consequent dissolution of its matrix and obtaining nanoparticles from the minor element [13, 14]. Nickel produced by this way is also called the Raney nickel. It is popular in catalysis due to large surface and also due to presence of hydrogen in the nickel. The properties of prepared nanoparticles as well as progress of the leaching process depend on initial alloy and also on leaching temperature. It was proven that gas-atomized powders are sufficient due to their small granulometry and also non-equilibria phase composition [15].

Magnetic properties of Raney nickel differ based on preparation route. One possible explanation is presence of various amount of residual aluminium in the product [2, 3]. It was already proven that this is not the only reason and grain size of nickel particles also plays crucial role [16].

The presence of hydrogen, which was proven in nickel particles, can help the catalytic ability. It provides to the nickel particles also feasibility of hydrogen storage. On the other hand, it is disadvantageous in powder metallurgy. The aim of this article was to describe influence of leaching temperature on Ni particles structure, properties and hydrogen intake.

Experimental

The master alloy with compositions of Al-50 wt.% Ni (32 at.% Ni) was prepared by gas atomization process. The rapidly solidified powder alloy was leached in 20 % (wt.) solution of NaOH, following this reaction scheme: (1)

$$\mathrm{Al(Ni) + 2\,NaOH + 6\,H_2O \rightarrow 2\,Na[Al(OH)_4] + 3\,H_2 (+ Ni)} \quad (1)$$

The nickel nanoparticles were prepared by selective leaching at different temperature: – 20, 0, 20, 40, 60 and 80 °C. Leaching at 0–80 °C was performed using magnetic stirring and heating device, while leaching at – 20 °C took place in cryostatic cell with mechanical stirring. The leaching was performed for 3 h at high temperatures (40–80 °C), 2 days at middle temperatures (0–20 °C) and 14 days at the lowest temperature (– 20 °C). The 20 % concentration of NaOH solution was chosen, since it enables to work at wide range of temperatures (determined by the freezing point of the solution), as shown in Fig. 1 [17].

The microstructure of nanoparticles was observed by scanning electron microscope TESCAN VEGA 3 LMU operated at 20 kV equipped by EDS detector (Oxford Instruments) and by transmission electron microscope Jeol JEM 3010 operated at 300 kV (LaB_6 cathode, point resolution = 1.7 Å). Particle- and grain-size were determined using image analysis software Image J.

Small angle neutron scattering measurements were done at the Budapest Research Reactor SANS instrument, called Yellow Submarine. The samples were measured in the form of uni-axialy pressed powders into a cylinder with 10 mm diameter and height of 3 mm. The whole covered Q range was: 0.008–0.4 $Å^{-1}$

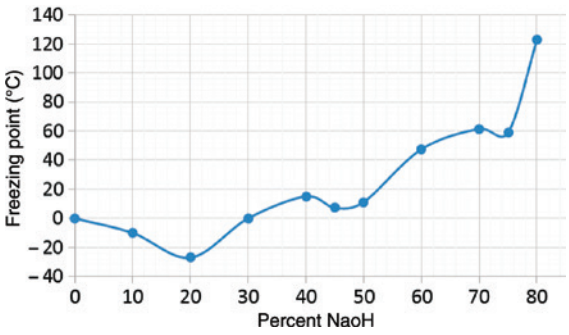

Fig. 1: NaOH solution freezing point dependence on NaOH concentration (given in wt.%) [17].

($Q = 4\pi\sin 2\theta/\lambda$). The Q range 0.008–0.02 $Å^{-1}$ corresponded to 11.61 Å wavelength and 5.4 m sample to detector distance, the 0.002–0.08 $Å^{-1}$ corresponded to 4.88 Å and 5.4 m, the 0.08–0.4 $Å^{-1}$ corresponded to 4.88 Å and 1.3 m.

Phase composition of initial materials and prepared nanoparticles was determined by X-ray diffraction (PANanalytical X'Pert PRO + High Score Plus, Co Kα radiation, 2Θ range of 20–140°). The crystallite size was obtained by evaluation of peak broadening by Rietveld analysis.

Magnetic properties of the powder samples were measured at room temperature by vibrational magnetometer PAR 4500 in form of air-dried powder. Partial oxidation took part during the drying process. So the magnetization measurements were repeated by measuring in small plastic cuvettes filled and dried in a glovebox. Subsequently the magnetic properties were characterized by Physical Property Measurement System (PPMS, Quantum Design).

The thermogravimetric measurements as well as measurements of amount of released hydrogen were performed by Setsys Evolution 1750 TG-DTA-MS Setaram, STA-EGA + Quadrupole MS Omnistar Pfeiffer. There was used about 50 mg of particles in isopropanol for one measurement that were subsequently dried in inert atmosphere to a constant weight, which was 14–19 mg. For estimation of released hydrogen amount the peaks of weight 1.1 and 2.1 (A) were integrated.

Results and discussion

The nickel nanoparticles were prepared by selective leaching at different temperature – 20, 0, 20, 40, 60 and 80 °C. The size of prepared nickel particles is given in Table 1 and it is obvious that the influence of leaching on the particle size is negligible. The particles are dendritic and have internal microstructure formed by crystalline grains separated by high angle grain boundaries. It was already shown [16] that the size of crystallite depends on leaching temperature. The dendritic-shaped particles are agglomerated in the clusters. It was published [15] that dendritic shape of Raney nickel origins from dendritic microstructure of initial Al–Ni gas-atomized alloy. Our previous studies on Al–Ni [16] and Al–Ag [11] alloys prepared by melt spinning and consequently subjected to selective leaching shown that dendritic particles are formed independently on the microstructure of initial alloy.

The results from HRTEM observation and XRD are in a good agreement and they show that at low leaching temperature small grains are formed and their size increases with increasing temperature, see Table 1. The microstructure of particles prepared at 0 °C is shown in Fig. 2.

The results obtained by microscopy and XRD are compared with results from small angle scattering.

The 2D scattering maps do not show any anisotropy in the bulk structure. Therefore the SANS curves were radially averaged, and the scattered and calibrated intensities were plotted versus the scattering vector Q. The obtained curves can be devided in two different regions (Fig. 3): the smaller Q region gives a so-called Guinier scattering from particles of size Rg_1, the larger Guinier region gives a Guinier scattering from particles of size Rg_2, and additionally to this we obtain a scattering from larger surfaces, that can be characterized with the so-called Power-law exponent.

Table 1: Average particle and grain sizes (given in nm) determined by image analysis and by XRD.

Temperature (°C)	Particle size (TEM)	Grain size (TEM)	Grain size (XRD)
– 20	240	4.99 ± 1.33	3.89
0	270	4.06 ± 1.01	3.95
20	240	4.18 ± 1.54	3.76
40	210	5.68 ± 1.18	4.08
60	240	6.17 ± 1.45	6.05
80	280	9.01 ± 2.46	6.43

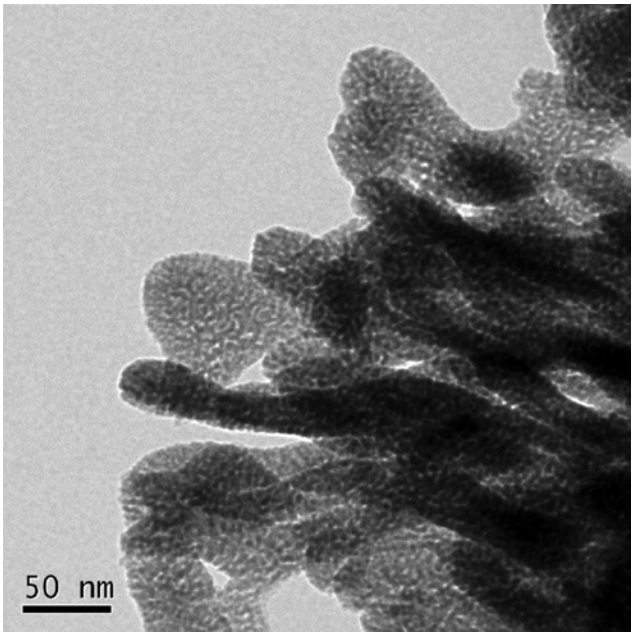

Fig. 2: Microstructure of nickel powder prepared by selective leaching at 0°.

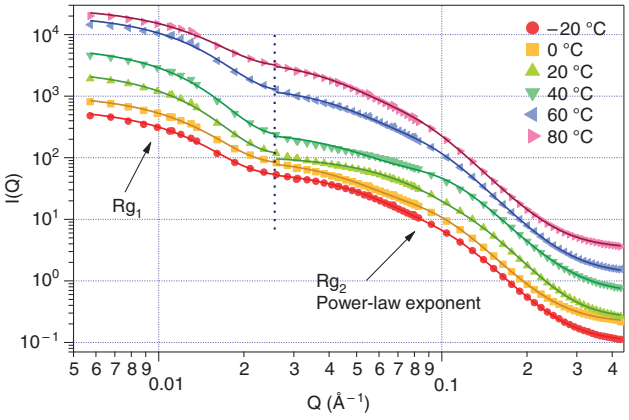

Fig. 3: SANS scattering curves of the nickel samples, prepared at different temperatures. The straight lines represent the fitted models. The curves are offset.

The fitting functions were the following:

$$\text{Smaller Q range, Guinier model: } I(Q) = A\exp\left(\frac{-Q^2Rg_1^2}{3}\right)$$

$$\text{Larger Q range: } I(Q) = B\exp\left(\frac{-Q^2Rg_2^2}{3}\right) + C\left(\frac{Q}{\text{erf}(QRg_2/\sqrt{6})}\right)^{-p}$$

where A, B, C are constant values of samples macroscopical features and instrument characteristics. SANS scattering curves of the nickel are given in Fig. 3.

Q is the scattering vector, Rg_1 and Rg_2 are radii of gyration, p is the power-law exponent. The values for the Rg_1, Rg_2 and p are listed in Table 2.

Table 2: Radii of gyration (Rg_1 and Rg_2) and power-law exponent (p) obtained by fitting of SANS curves.

Temperature (°C)	Rg1 (Å) ± err of the fit	Rg2 (Å) ± err of the fit	p ± err of the fit
– 20	158.1 ± 0.4	32.34 ± 0.07	4.61 ± 0.01
0	155.3 ± 0.4	35.14 ± 0.08	4.56 ± 0.01
20	161.3 ± 0.3	24.02 ± 0.03	5.14 ± 0.01
40	161.4 ± 0.3	33.20 ± 0.06	4.44 ± 0.01
60	151.5 ± 0.3	37.32 ± 0.09	4.53 ± 0.01
80	146.6 ± 0.5	40.45 ± 0.10	4.58 ± 0.01

Two sets of different sized scattering objects were detected in the bulk structure of the samples: the smaller size is approximately between 50 Å and 80 Å diameter (Rg_2), the larger (Rg_1) is around 300 Å. The most probable explanation is that Rg_2 value is coming from the crystalline grains, while the Rg_1 value corresponds to the residual porosity originated from uni-axial presing of the particles into tablets. A fact prooving this theory is that by measuring the powder sample in a glass cuvette only one radius of gyration was observed [16].

Additionally a power-law exponent can be obtained from the larger Q range fit (the Guinier model alone did not fit the measured data), which value is above 4, for every sample. A steep power-law scatteirng slope can be attributed to a gradual scattering length density change on the limit of large surfaces. Previously the power-law exponent above 4 has been observed for the crystalline-amorphous surfaces with a gradual density change. As the samples are analyzed after drying the explanation of p value is in presence of thin oxide layer on the surface of particles.

The exceptional behavior of sample prepared by leaching at 20 °C can be probably explained by partial oxidation of the sample during drying process which cannot be fully omited.

The grain sizes of Ni particles obtained by above mentioned methods (HRTEM, XRD and SANS) are summarized in Fig. 4.

High reactivity of samples prepared at 20 and 40 °C is also documented by measuring of magnetic properties on dried samples. The curves given in Fig. 5 show very different behavior for these two samples. As the saturated magnetization is significantly lower, the reason is oxidation of the samples. Based on this experience, the magnetization measurements for selected samples was repeated by measuring the samples in small plastic cuvettes dried in a glovebox that prevented the samples from oxidation. The curves in Fig. 6 shows dependence of saturated magnetization on leaching temperature as it is increasing with increasing leaching temperature. While the value of saturated magnetization for sample prepared at 80 °C is lower than that prepared at 60 °C, it might be hint for some contamination of the sample (or partial oxidation). All samples

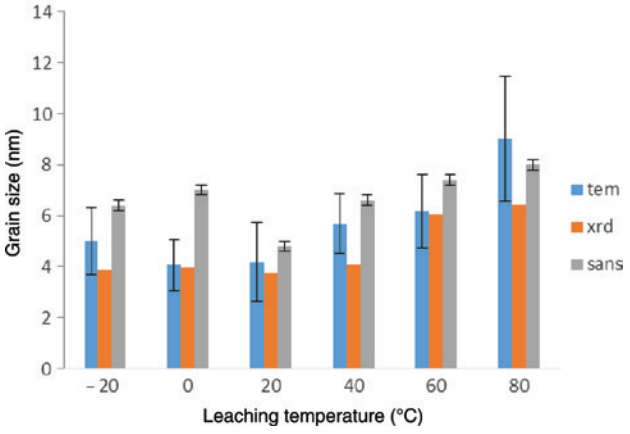

Fig. 4: Comparison of nickel grain sizes obtained by TEM, XRD and SANS.

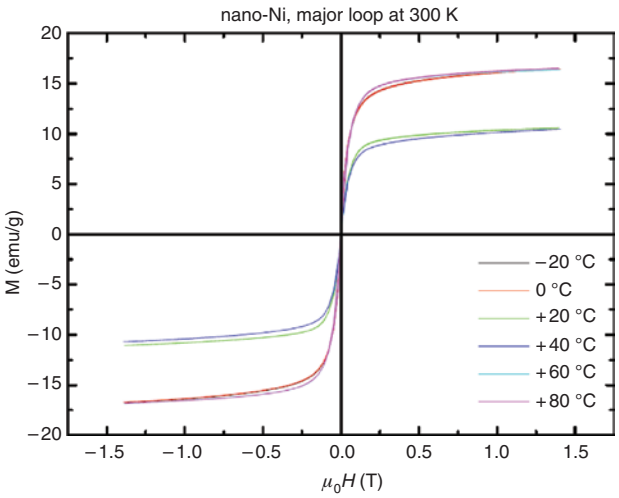

Fig. 5: Magnetization curves of nickel nanoparticles prepared by selective leaching at – 20, 0, 20, 40, 60 and 80 °C measured on air-dried powder.

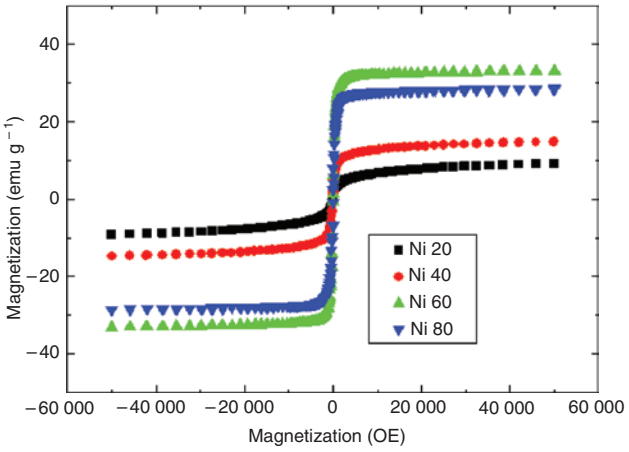

Fig. 6: Magnetization curves of nickel nanoparticles prepared by selective leaching at 20, 40, 60 and 80 °C measured in plastic cuvette and dried in glovebox in inert gas.

had significantly lower saturated magnetization than standard material (electolytical Ni, saturated magnetization 57 emu/g). It confirms the results from HRTEM, XRD and SANS showing very fine structure of particles formed by grains with size of few nanometers. The reason for suppression of saturated magnetization is in so called "dead zones" [18]. These are areas of grain boundaries where the structure is deformed and, therefore they do not contribute to ferromagnetic behavior of the material. The decrease in saturated magnetization value was also proven for chemically reduced nickel nanoparticles [12]. The authors obtained saturated magnetization of 22 emu/g for nanoparticles with size of 9.2 nm. This result is in a good agreement with ours.

Based on thermogravimetric measurement accompanied by mass-spectroscopy, the hydrogen was released from particles between 80 and 150 °C. It is a big advantage compared to hydrazine reduction, where the hydrogen is released during the process of nickel particles formation [12]. In case of nickel particles prepared by selective leaching method, hydrogen is stored until heating up of the particles. The curves shown in Fig. 7 indicate that for samples leached at higher temperature more hydrogen is released at lower temperatures but the effect is not significant. The amount of released hydrogen was about 1.5 wt.% independently on sample preparation. Hydrogen is created and enters nickel particles during dissolution of Al matrix. The ratio of Ni and Al is the same for all the samples. The same amount of hydrogen trapped in Ni particles illustrates

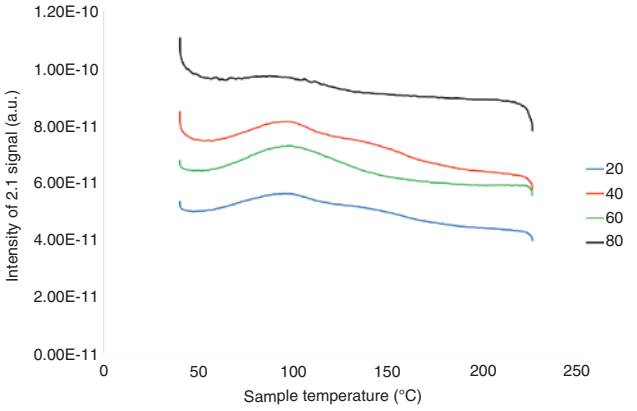

Fig. 7: TG-DTA-MS curves showing the hydrogen release (as 2.1 mass weight peak) from nickel nanoparticles prepared by selective leaching at 20, 40, 60 and 80 °C.

that there is no kinetic problem of hydrogen intake although at higher leaching temperatures the process runs faster.

Conclusion

The results given in this article shows that the microstructure of Ni particles prepared by selective leaching method from Al–Ni alloy is dependent on temperature. While the size of the particles remains approximately the same (about 250 nm), the size of grains forming the particles increase with increasing leaching temperature. This behavior was proven by HRTEM observation, analysis of peak broadening in XRD and by small angle neutron scattering.

Magnetic properties derive from the grain size of polycrystalline material. So with decreasing leaching temperature (decreasing grain-size) the value of saturated magnetization decreases.

The amount of hydrogen released from nickel particles by heating is independent on leaching temperature.

Acknowledgments: Alena Michalcová, Dalibor Vojtěch and Ivo Marek thank for financial supported by Czech Science Foundation, project No. P108/12/G043. Adél Len thanks for support by the European Commission under the 7th Framework Programme through the Key Action: Strengthening the European Research Area, Research Infrastructures. Grant Agreement N 283883-NMI3-II.

References

[1] N. Toshima. *Pure Appl. Chem.* **85**, 437 (2013).
[2] P. Fouilloux, G. A. Martin, A. J. Renouprez, B. Moraweck, B. Imelik, M. Prettre. *J. Catal.* **25**, 212 (1972).
[3] P. Fouilloux. *Appl. Catal.* **8**, 1 (1983).
[4] F. Wang, Z. Zhang, Z. Chang. *Mater. Lett.* **55**, 27 (2002).
[5] D. E. Zhang, X. M. Ni, H. G. Zheng, T. Y. Li, X. J. Zhang, Z. P. Yang. *Mater. Lett.* **59**, 2011 (2005).
[6] Ch. Jiang, G. Zou, W. Zhang, W. Yu, Y. Qian. *Mater. Lett.* **60**, 2319 (2006).
[7] L. Bai, F. Yuan, Q. Tang. *Mater. Lett.* **62**, 2267 (2008).
[8] H. Hu, K. Sugawara. *Mater. Lett.* **62**, 4339 (2008).
[9] P. K. Khanna, P. V. More, J. P. Jawalkar, B. G. Bharate. *Mater. Lett.* **63**, 1384 (2009).
[10] L. Zhao, Y. Wang, Q. Jiang. *Mater. Lett.* **64**, 215 (2010).
[11] I. Marek, D. Vojtech, A. Michalcova, T. F. Kubatik. *Mater. Sci. Eng. A* **627**, 326 (2015).
[12] S. Wu, D. Chen. *J. Colloid Interf. Sci.* **259**, 282 (2003).
[13] D. Vojtěch, A. Michalcová, M. Klementová, J. Šerák, M. Mort'aniková. *Mater. Lett.* **63**, 1074 (2009).

[14] O. Milkovič, G. Janák, Š. Nižník, S. Longauer, L. Fröhlich. *Mater. Lett.* **64**, 144 (2010).
[15] F. Devret, G. Reinhart, G. N. Iles, B. van der Klugt, N. J. Adkins, J. W. Bakker, B. E. Nieuwenhuys. *Catal. Today* **163**, 13 (2011).
[16] A. Michalcova, P. Svobodova, R. Novakova, A. Len, O. Heczko, D. Vojtech, I. Marek, P. Novak. *Mater. Lett.* **137**, 221 (2014).
[17] http://www.puritanproducts.com/wp-content/uploads/2015/09/Sodium-Hydroxide-Freezing-Points-Chart.png (17.9.2016).
[18] L. Liebermann, J. Clinton, D. Edwards, J. Mathon. *Phys. Rev. Lett.* **25**, 232 (1970).